Chin. J. Astron. Astrophys. Vol. 3 (2003), No. 5, 478–490
(http://www.chjaa.org or http://chjaa.bao.ac.cn)

Chinese Journal of
Astronomy and
Astrophysics

A Study of the Fitting Accuracy of the Active Reflector for a Large Spherical Radio Telescope *

Xiao-Qiang Tang[1], Jin-Song Wang[1] and Qi-Ming Wang[2]

[1] Department of Precision Instruments, Tsinghua University, Beijing, 100084;
tangxq@pim.tsinghuia.edu.cn
[2] National Astronomical Observatories, Chinese Academy of Sciences, Beijing, 100012

Received 2003 March 21; accepted 2003 April 22

Abstract We propose a spatial three-degree-of-freedom (DOF) parallel mechanism combining two degrees of rotations and one degree of translation to support the active reflector units of a large spherical radio telescope. The kinematics, workspace and accuracy of the mechanism are analyzed. One-dimensional and two-dimensional fitting errors to the working region of active reflector are investigated. Dimensional parameters of the mechanism and active reflector unit are examined with respect to the requirement of fitting accuracy. The result of accuracy analysis shows the effectiveness and feasibility of the proposed mechanism, and gives a design rule to guarantee the highest working frequency required by large radio telescope.

Key words: telescopes: radio telescope — active reflector

1 INTRODUCTION

Since radio telescopes are the main tool for human kind to search for the universe's secret, astronomers reached unanimity at the 24th URSI Conference in Kyoto, Japan, in 1993, and proposed to construct the next generation of large radio telescope (LT) (Nan et al. 2000). From then on, astronomers of China have begun a project of Five-hundred meter Aperture Spherical radio Telescope (FAST) as the prototype of the LT (Large Radio Telescope) (Qiu 1998; Peng et al. 2000; Li 1998).

It is well known that the Arecibo telescope was a breakthrough in the building of large radio telescopes. Its main mirror, 305 m in diameter, is fixed on a karst base, and an elaborately designed feed system illuminates a part of the mirror which forms an effective aperture of about 200 m. The feed system is movable at a height of about 100 m when tracking the object to be observed. The enormous receiving area of the telescope will enable it to make many important astronomical discoveries inaccessible to lesser instruments, despite its limited sky coverage (20° zenith scan angle) due to geometrical configuration, and its narrow frequency bandwidth, originated from spherical aberration. An upgrade project has been carried out for

* Supported by the National Natural Science Foundation of China.

the Arecibo telescope, in which a heavy and complex hence expensive Gregorian dual-reflector feed system is introduced for correcting the spherical aberration and enlarging the bandwidth (Duan 1999).

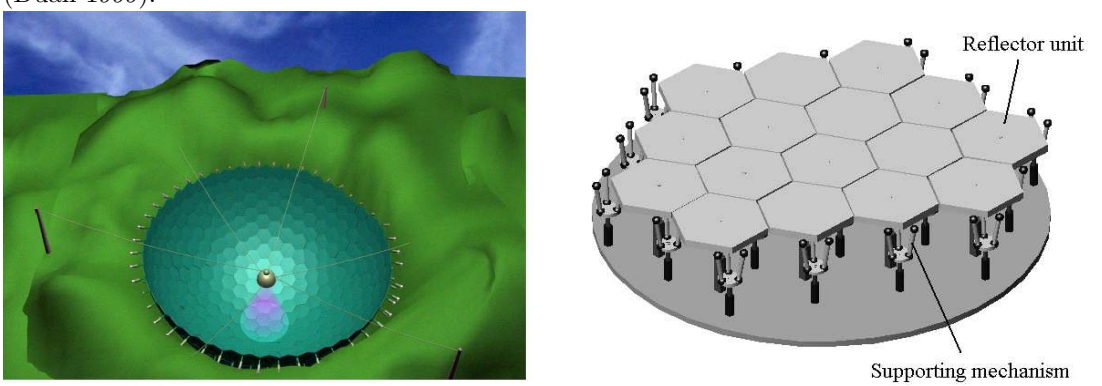

(a) (b)

Fig. 1 Active reflector of spherical radio telescope. (a) A Bird's-eye view of project FAST; (b) Reflector units with supporting mechanism

For the sake of satisfying the requirements of low cost and broad bandwidth, the project group of FAST decided to substitute the fixed spherical reflector with active reflector units. As shown in Fig. 1, the reflector consists of about 2000 elementary reflector units. Figure 1b shows some of the active reflector units and supporting mechanisms. Each reflector unit is a small part of a spherical surface of regular hexagon and is driven by a supporting mechanism. The part of spherical reflector illuminated by the feed is continuously adjusted to fit a paraboloid of revolution in real-time, synchronous with the motion of the feed while tracking the object to be observed (Qiu 1998). As it is now free from spherical aberration, a simple, light-weight, hence cheap feed system may be adopted to achieve broad bandwidth and full polarization. In order to fit a paraboloid of revolution, it is necessary that every reflector unit should be driven by a supporting mechanism with two rotational degrees of freedom and one translational degree of freedom (Luo et al. 2000). The mechanism will bring error because of the control or dimensional factor. Moreover, the fitting surface of reflector will not match exactly the nominal paraboloid. In order to guarantee the working frequency of the large spherical radio telescope, the fitting accuracy of the active reflector should be studied systematically.

In this paper, a new supporting mechanism for the active reflector units is proposed, which is based on a 3-PSS parallel mechanism with a passive leg. The movable platform of the parallel mechanism has three degrees of freedom, two in orientation and one in translation, with respect to the base plate. Based on the analysis of the kinematics and error of the mechanism, the one dimensional and two dimensional fitting errors to the active reflector working region are investigated systematically.

2 DESCRIPTION OF SUPPORTING MECHANISM

To adjust the reflector units to fit a paraboloid, a new type of parallel supporting mechanism is proposed as shown in Fig. 2, which is based on a 3-PSS parallel mechanism with a passive leg. The parallel supporting mechanism consists of a base plate, a movable platform, and four connecting legs, three of which have identical kinematic chains, PSS. Each of the three legs is

composed of one fixed length link (3), and one union driven plate (5). The fixed length link (3) is connected to the movable platform (1) and the union driven plate (5) by two spherical joints (2) and (4), respectively. The union driven plate (5) is connected to the base plate (5) by a prismatic joint (6). The base plate and the movable platform are two regular triangles. The passive leg (8) connects the center points of the two regular triangles. One end of the passive leg has a 2-DOF universal joint (6), the other one is fixed to the base plate (5) by a prismatic joint (7). The passive leg (8) can be extensible with the prismatic joint (7) along its axis line. Furthermore, when the supporting mechanism is assembled, the axis line of the prismatic joint (7) should pass the center of the spherical reflector. Since a supporting mechanism should be driven by three actuator legs, as shown in Fig. 2, the union driven plate (5) connects three fixed length links in order to reduce the actuator number. As a result, the number of actuators of the active reflector is equal to that of the reflector units.

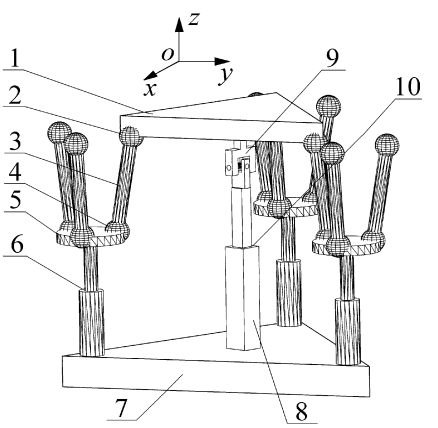

Fig. 2 Parallel supporting mechanism.

As described above, one can see that the proposed mechanism is one of n DOFs, which usually consists of n identical actuated legs with six DOFs and one passive leg with n DOFs connecting the movable platform and the base plate, i.e., the DOF of the mechanism is dependent on the passive leg's DOF. For the mechanism considered in this paper, the passive leg has three DOFs, which means n equals 3. The three DOFs are one of translation along the z axis and two of rotation about the x and y axes.

3 KINEMATICS ANALYSIS

Mechanism kinematics deals with the study of the mechanism's motion as constrained by the geometry of the links. Typically, the study of mechanism kinematics can be divided into two parts, inverse kinematics and forward (or direct) kinematics (Wang et al. 2003). The inverse kinematics involves mapping a known pose (position and orientation) of the output platform of the mechanism to a set of input joint variables that will achieve that pose. The forward kinematics involves the mapping from a known set of input joint variables to a pose of the movable platform that results from those given inputs (Wang et al. 2001). Generally, as the number of closed kinematics loops in the parallel mechanism increases, the difficulty of solving the forward kinematics relationships increases, while the difficulty of solving the inverse kinematics relationships decreases (Liu et al. 2001; Wang et al. 2003).

3.1 Inverse Kinematics

A kinematics model of the mechanism is developed as shown in Fig. 3. The vertices of the movable platform are denoted as platform joints A_i $(i = 1,\ 2,\ 3)$, and the vertices of the base plate are denoted as b_i $(i = 1,\ 2,\ 3)$. A fixed global reference system $\Re{:}o - xyz$ is located at the center of the regular triangles $b_1b_2b_3$ with the axis z normal to the base plate and the axis y parallel to the side b_1b_2. The circumcircle radius of triangles $b_1b_2b_3$ is denoted as R. Another reference frame, called the top frame $\Re'{:}o' - x'y'z'$, is located at the center of regular triangles $A_1A_2A_3$. The axis z' is perpendicular to the movable platform and y' axis parallel to the side A_1A_2. The circumcircle radius of triangles $A_1A_2A_3$ is denoted as r. Vectors of fixed length links are denoted as $\mathbf{L}_i$ $(i = 1,\ 2,\ 3)$, and the link length for each legs is denoted as l, where $A_iB_i = l$, $(i = 1,\ 2,\ 3)$.

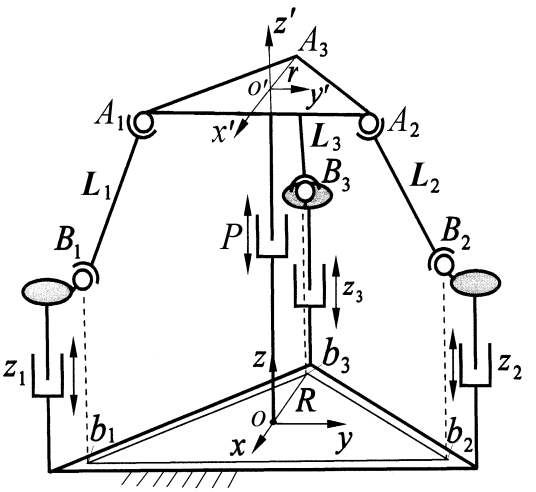

Fig. 3 Geometric parameters of the parallel mechanism.

The task of the inverse kinematics solution is to define a mapping from the pose of the output platform in Cartesian space to the set of actuated inputs that achieve that pose. For this analysis, the pose of the movable platform is considered known, and the position is given by the position vector $[\mathbf{o}']_{\Re}$ and the orientation is given by a matrix $\mathbf{R_1}$. Then we have

$$[\mathbf{o}']_{\Re} = \begin{pmatrix} x & y & z \end{pmatrix}^{\mathrm{T}}, \tag{1}$$

where $x = y = 0$,

$$\mathbf{R}_1 = \begin{bmatrix} c\beta & s\beta s\alpha & s\beta c\alpha \\ 0 & c\alpha & -s\alpha \\ -s\beta & c\beta s\alpha & c\beta c\alpha \end{bmatrix}, \tag{2}$$

where c stands for the cosine function, s, the sine function, α and β are the orientational DOFs of the movable platform with respect to the x and y axes, respectively. The coordinate of point A_i in the frame $\Re'$ can be described by the vector $[\mathbf{A}_i]'_{\Re}$ $(i = 1,\ 2,\ 3)$, and

$$[\mathbf{A_1}]_{\Re'} = \left[r/2, -\sqrt{3}r/2, 0\right]^{\mathrm{T}}, \quad [\mathbf{A_2}]_{\Re'} = \left[r/2, \sqrt{3}r/2, 0\right]^{\mathrm{T}}, \quad [\mathbf{A_3}]_{\Re'} = [-r, 0, 0]^{\mathrm{T}}. \tag{3}$$

Vectors $[\mathbf{B}_i]_{\Re}$ $(i = 1,\ 2,\ 3)$ will be defined as position vectors of base joints B_i in frame $\Re$, and

$$[\mathbf{B_1}]_{\Re} = \left[R/2, -\sqrt{3}R/2, z_1\right]^{\mathrm{T}}, \quad [\mathbf{B_2}]_{\Re} = \left[R/2, \sqrt{3}R/2, z_2\right]^{\mathrm{T}}, \quad [\mathbf{B_3}]_{\Re} = [-R, 0, z_3]^{\mathrm{T}}\ . \quad (4)$$

Vectors $[\mathbf{A}_i]_{\Re}$ $(i = 1,\ 2,\ 3)$ in frame $o - xyz$ can be, therefore, written as

$$[\mathbf{A}_i]_{\Re} = \mathbf{R}_1\,[\mathbf{A}_i]'_{\Re} + [\mathbf{o}']_{\Re}\ . \qquad (i = 1, 2, 3) \quad (5)$$

Then the inverse kinematics of the parallel mechanism can be solved by writing the following constraint equation

$$\|[\mathbf{B}_i]_{\Re} - [\mathbf{A}_i]_{\Re}\| = \|\mathbf{L}_i\| = l\,. \qquad (i = 1, 2, 3) \quad (6)$$

Hence, for a given mechanism and a prescribed position and orientation of the movable platform, the required actuator inputs can be directly computed from Eq. (6), that is

$$\begin{cases} z_1 = \sqrt{l^2 - A_{11}^2 - A_{12}^2} + A_{13} \\ z_2 = \sqrt{l^2 - A_{21}^2 - A_{22}^2} + A_{23} \\ z_3 = \sqrt{l^2 - A_{31}^2 - A_{32}^2} + A_{33} \end{cases}, \quad (7)$$

where

$$\begin{aligned} A_{11} &= (R - r(c\beta - \sqrt{3}s\beta s\alpha))/2 \\ A_{12} &= -\sqrt{3}(R - rc\alpha)/2 \\ A_{13} &= r(s\beta + \sqrt{3}c\beta s\alpha)/2 + z \\ A_{21} &= R - r(c\beta + \sqrt{3}s\beta s\alpha)/2 \\ A_{22} &= \sqrt{3}(R - rc\alpha)/2 \\ A_{23} &= -r(s\beta - \sqrt{3}c\beta s\alpha)/2 + z \\ A_{31} &= -R + rc\beta \\ A_{32} &= 0 \\ A_{33} &= rs\beta + z \end{aligned} \quad ,$$

3.2 Forward Kinematics

The task of the forward kinematics solution is to define a mapping from the known set of the actuated inputs to the unknown pose of the output platform. For the architecture with prismatic actuators, the inputs that are considered known are the lengths of the three actuator legs z_1, z_2 and z_3. The unknown pose of the output platform is described by the position vector $[\mathbf{o}']_{\Re}$ and angles α and β. Because it is very difficult to describe the direct kinematics in closed form for this type of parallel mechanism, the forward kinematics solution should be obtained by numerical methods as follows:

(1) Decide the non-singular workspace of the mechanism;
(2) Give the initial value of the direct kinematics solution;
(3) Calculate the position coordinates of spherical joints, construct the nonlinear equations set by the geometrical constraints of the fixed length links;
(4) Solve the nonlinear equations set by the Quasi-Newton method (Press et al. 1995).

From Eq. (6), the nonlinear equation is

$$f_i\,(z, \alpha, \beta) = l^2 - A_{i1}^2 - A_{i2}^2 - (z_i - A_{i3})^2 = 0, \qquad (i = 1, 2, 3) \quad (8)$$

where the direct kinematics solutions are z, α and β.

3.3 Velocity Equation

Equation (6) can be differentiated with respect to time to obtain the velocity equation. This leads to the equation

$$\mathbf{J}_p\dot{\mathbf{p}} = \mathbf{J}_q\dot{\mathbf{q}} \quad , \tag{9}$$

where $\dot{\mathbf{q}}$ is the vector of Cartesian velocities defined as

$$\dot{\mathbf{q}} = \left[\dot{z}, \dot{\alpha}, \dot{\beta}\right]^{\mathrm{T}}, \tag{10}$$

and $\dot{\mathbf{p}}$ is the vector of input velocities defined as

$$\dot{\mathbf{p}} = [\dot{z}_1, \dot{z}_2, \dot{z}_2]^{\mathrm{T}}. \tag{11}$$

Matrices $\mathbf{J}_p$ and $\mathbf{J}_q$ are the 3×3 forward and inverse Jacobian matrices of the mechanism and can be expressed as

$$\mathbf{J}_p = \begin{bmatrix} (z_1 - A_{13})/l & 0 & 0 \\ 0 & (z_2 - A_{23})/l & 0 \\ 0 & 0 & (z_3 - A_{33})/l \end{bmatrix} \quad , \tag{12}$$

$$\mathbf{J}_q = \begin{bmatrix} (\mathbf{w}_1)_z & (\mathbf{v}_1 \times \mathbf{w}_1)_x & (\mathbf{v}_1 \times \mathbf{w}_1)_y \\ (\mathbf{w}_2)_z & (\mathbf{v}_2 \times \mathbf{w}_2)_x & (\mathbf{v}_2 \times \mathbf{w}_2)_y \\ (\mathbf{w}_3)_z & (\mathbf{v}_3 \times \mathbf{w}_3)_x & (\mathbf{v}_3 \times \mathbf{w}_3)_y \end{bmatrix} \quad , \tag{13}$$

where $\mathbf{w}_i$ is the unit vector of $\mathbf{L}_i$, and $\mathbf{v}_i = \mathbf{R}_1 \left[\mathbf{A}_i\right]_{\Re'}$, $(\mathbf{w}_i)_z$ is the element of vector $\mathbf{w}_i$ with respect to z axis coordinate, $(\mathbf{v}_i \times \mathbf{w}_i)_x$ and $(\mathbf{v}_i \times \mathbf{w}_i)_y$ are the elements of vector $\mathbf{v}_i \times \mathbf{w}_i$ with respect to x and y axis coordinates, respectively.

4 MECHANISM ACCURACY ANALYSIS

When the large spherical radio telescope is running, the part of the spherical reflector illuminated by the feed is continuously adjusted to fit a paraboloid of revolution in real-time, synchronous with the motion of the feed when tracking the object observed. The spherical surface reflector is divided into some small elementary units. When the mechanisms drive the reflector units to fit the paraboloid, the fitting surface of reflector will not match exactly the nominal paraboloid. Moreover, the mechanism produces errors because of some control or dimensional factor. In this section we first analyze the mechanism accuracy.

The mechanism accuracy involves the error caused by the actuator input error and the joint error of the mechanism. The actuator input error is denoted as $\delta\mathbf{p} = [\delta z_1, \delta z_2, \delta z_3]^{\mathrm{T}}$ and the joint error is denoted as $\delta\mathbf{e} = \left[\ \delta\mathbf{A}_i^{\mathrm{T}}\ \ \delta\mathbf{B}_i^{\mathrm{T}}\ \right]^{\mathrm{T}} \in R^{18\times1}(i = 1, ...3)$, where $\delta\mathbf{B}_i^{\mathrm{T}} \in R^{9\times1}(i = 1, ...3)$ includes the joint error on the base platform and the input error $\delta\mathbf{p} = [\delta z_1, \delta z_2, \delta z_3]^{\mathrm{T}}$. The output error is denoted as $\delta\mathbf{q} = [\delta z, \delta\alpha, \delta\beta]^{\mathrm{T}}$.

From Eqs. (5) and (6), the inverse kinematics equation can be written as

$$\mathbf{R}_1 \left[\mathbf{A}_i\right]_{\Re'} + \left[\mathbf{o}'\right]_{\Re} - \left[\mathbf{B}_i\right]_{\Re} = \mathbf{L}_i = \mathbf{w}_i l \,. \tag{14}$$

Differentiating Eq. (14) leads to

$$\delta\mathbf{l} = \mathbf{J}_q\delta\mathbf{q} + \mathbf{J}_e\delta\mathbf{e} \,, \tag{15}$$

where

$$\mathbf{J}_e = \begin{bmatrix} \mathbf{w}_1^{\mathrm{T}}\mathbf{R}_1 & -\mathbf{w}_1^{\mathrm{T}} & 0 & 0 & 0 & 0 \\ 0 & 0 & \mathbf{w}_2^{\mathrm{T}}\mathbf{R}_1 & -\mathbf{w}_2^{\mathrm{T}} & 0 & 0 \\ 0 & 0 & 0 & 0 & \mathbf{w}_3^{\mathrm{T}}\mathbf{R}_1 & -\mathbf{w}_3^{\mathrm{T}} \end{bmatrix} \in R^{3\times 18}, \tag{16}$$

and $\delta\mathbf{l} = [\delta l_1, \delta l_2, \delta l_3]^{\mathrm{T}}$, $\delta l_i (i = 1, 2, 3)$ is the manufacturing or measuring error of the ith link. When $\mathbf{J}_q$ is nonsingular in the workspace, Eq. (12) can be rewritten as

$$\delta\mathbf{q} = \mathbf{J}_q^{-1} \left(\delta\mathbf{l} - \mathbf{J}_e \delta\mathbf{e}\right) . \tag{17}$$

5 FITTING ACCURACY ANALYSIS OF ACTIVE REFLECTOR

5.1 One Dimensional Fitting Accuracy Analysis

As shown in Fig. 4, the base active reflector of the radio telescope is a spherical surface with a 500-meter aperture, and the working reflector is a paraboloid with a 300-meter aperture. When it works, the reflector units are driven by the parallel mechanism from the initial position to the fitting position to fit the paraboloid. Because the paraboloid is formed by the revolution of a parabola, we can analyze the deviation between spherical surface and paraboloid in the reflector frame $\Re'':o'' - y''z''$, which is built as shown in Fig. 4, where the spherical surface and the paraboloid in the frame $\Re''$ are circular arc and parabola, respectively.

Figure 5 shows one reflector unit which is in the initial position and fitting position, respectively. The initial position is located at the base spherical reflector surface. The deviation from the circular arc to the parabola is denoted as ΔK_{ij}, and suffix i represents the ith reflector unit which corresponds to the ith mechanism. The suffix $j (j = 1, 2, 3)$ represents the supporting point of the movable platform. The explanations of other symbols used in accuracy analysis are:

A_{ij} The supporting point when the reflector unit is in the initial position

A'_{ij} The supporting point while the reflector unit is in the fitting position

C_{ij} The intersecting points of line SA_{ij} and the parabola

o'_i The reference center in the movable platform while the reflector unit is in the initial position

o''_i The reference center in the movable platform while the reflector unit is in the fitting position

S The center of spherical reflector

K The radius of spherical reflector

F The focal point of the paraboloid

The absolute actuator input of the ith mechanism is specified as $\Delta K_{ij} (j = 1, 2, 3)$, while the ith active reflector unit is driven to fit the paraboloid. Obviously, the driven reflector unit will not match exactly the nominal paraboloid. In order to evaluate the fitting error, as shown in Fig. 5, Δe_i is defined as the deviation of center points of the ith reflector unit to the corresponding paraboloid and one-dimensional fitting error, and is equal to $\|o''_i C_{i3}\|$.

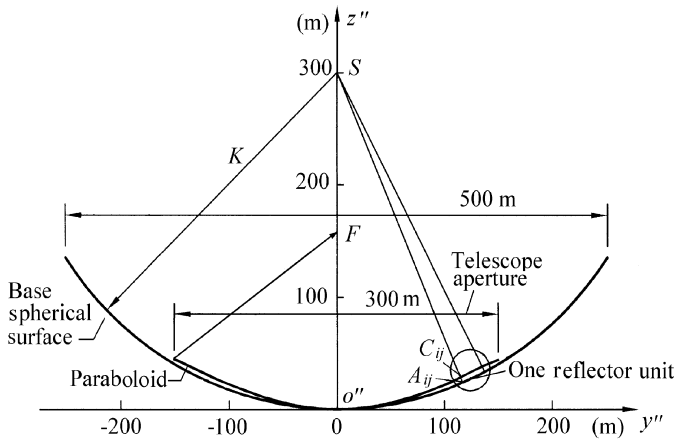

Fig. 4 Configuration of the active reflector.

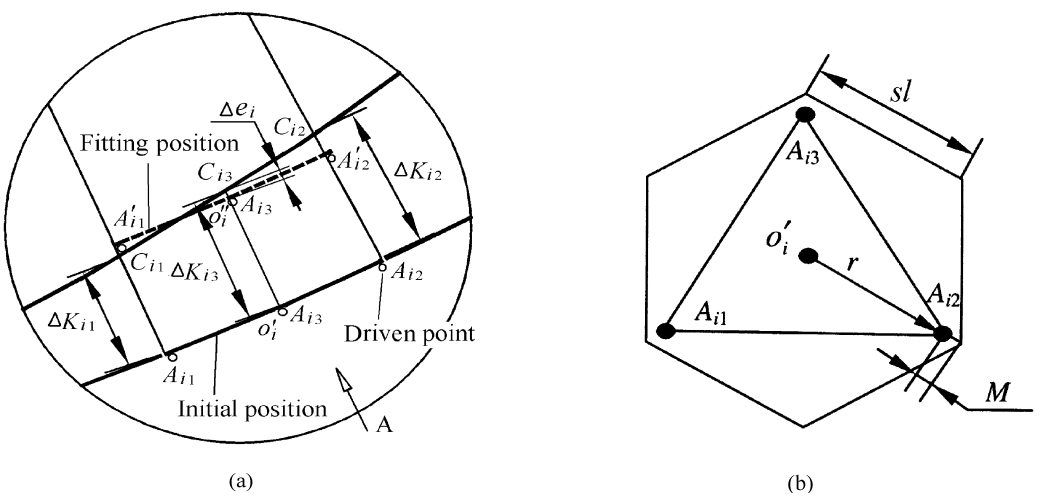

Fig. 5 ith reflector unit. (a) Initial and fitting position; (b) A direction view of initial position.

5.1.1 Parabola Equation and Circle Equation

According to (Qiu 1998), the focal length of the parabola is specified as $0.476K$, then the parabola equation can be written as

$$z'' = \frac{1}{4 \times 0.467K} y''^2 \quad . \tag{18}$$

The base spherical surface in reflector coordinate system $\Re''$ is a circle, and the circle equation can be written as

$$z'' = K - \sqrt{K^2 - y''^2}. \tag{19}$$

5.1.2 Actuator Input Range

The coordinate of the point A_{ij} in the frame $\Re''$ can be described by the vector $[\mathbf{A}_{ij}]''_{\Re}$ $(j = 1,\ 2,\ 3)$, then

$$[\mathbf{A}_{ij}]_{\Re''} = \left[y''_{ij}, z''_{ij}\right]^{\mathrm{T}}. \quad (j = 1, 2, 3) \tag{20}$$

The equation of straight line SA_{ij} can be written as

$$z'' = \frac{(z''_{ij} - K)y''}{y''_{ij}} + K. \quad (j = 1, 2, 3). \tag{21}$$

According to Eqs. (19) and (21), the point of intersection C_{ij} between line SA_{ij} and the circle can be expressed by the vector $[\mathbf{C}_{ij}]_{\Re''}$, which is

$$[\mathbf{C}_{ij}]_{\Re''} = [y''_{cij}, z''_{cij}]^{\mathrm{T}}. \quad (j = 1, 2, 3) \tag{22}$$

The actuator input value of the ith reflector unit can be written as

$$\Delta K_{ij} = \|K - SC_{ij}\| = K - \sqrt{(y''_{cij})^2 + (K - z''_{cij})^2}. \quad (j = 1, 2, 3) \tag{23}$$

5.1.3 One-Dimensional Fitting Error

When the actuator input ΔK_{ij} $(j = 1, 2, 3)$ is specified, the fitting error Δe_i can be reached. The first step is to calculate the position coordinate $[\mathbf{o}''_i]_{\Re} = [y, z]^{\mathrm{T}}_{\Re}$ in the frame $\Re$ by the forward kinematics solution. The position vector of the center point o''_i in the frame $\Re''$ is written as

$$[\mathbf{o}''_i]_{\Re''} = [y''_{o''i}, z''_{o''i}]^{\mathrm{T}} = \mathbf{R}_2\,[\mathbf{o}''_i]_{\Re} + [y''_{i3}, z''_{i3}]^{\mathrm{T}}, \tag{24}$$

where $\mathbf{R}_2$ is the rotation matrix about the frame $\Re{:}o - yz$ to the frame $\Re{:}o'' - y''z''$, i.e.,

$$\mathbf{R}_2 = \begin{bmatrix} c\alpha' & -s\alpha' \\ s\alpha' & c\alpha' \end{bmatrix}, \tag{25}$$

where $\alpha' = \sin^{-1}\left(\frac{y''}{K}\right)$. Then the fitting error is expressed as

$$\Delta e_i = So''_i - SC_{i3} = \sqrt{(y''_{o'i})^2 + (z''_{o'i} - K)^2} - \sqrt{(y''_{ci3})^2 + (z''_{ci3} - K)^2}. \tag{26}$$

Since the three-hundred-meter aperture paraboloid is composed of a large number of reflector units, we should analyse all the errors of all the reflector units. When the error is studied in the reflector frame $\Re''{:}o'' - y''z''$ and the side length of the reflector unit is specified, the one-dimensional root-mean-square (RMS) fitting error of the paraboloid reflector can be defined as

$$Re = \sqrt{\frac{\sum_{i=1}^{n} \Delta e_i^2}{n}}. \tag{27}$$

5.1.4 One-Dimensional Accuracy Synthesis Analysis

Accuracy synthesis analysis is defined as the combined RMS error of the errors of the mechanism actuator input and of the fitting. the former has a linear relationship with the value of ΔK_{ij}, and Eq. (23) can be rewritten as

$$\Delta K_{ij} = \|K - SC_{ij}\| + \delta z_j = K - \sqrt{(y''_{cij})^2 + (z''_{cij} - K)^2} + \delta z_j, \quad (j = 1, 2, 3) \tag{28}$$

where δz_j $(j = 1, 2, 3)$ is the actuator input error. Then Eqs. (24)–(27) can be used to calculate the one-dimensional composition RMS error $R'e$.

5.1.5 Simulation Example

Since the position of the supporting point A_{ij} should be limited in the range of the reflector unit, as shown in Fig. 5b, the base plate parameter r of the parallel mechanism is

$$r = sl - M\,, \tag{29}$$

where sl is the side length of the reflector unit and $M$is the distance from the movable platform edge to the reflector unit edge. In this work, $M = 0.5$m and $R = r = 2l$.

Since the paraboloid reflector is symmetrical, the error can be analyzed for the range of 150 m. Figure 6 shows the one-dimensional fitting error when the side length of reflector unit is specified.

According to Eqs. (26) and (28), the one-dimensional RMS fitting error and composition RMS error are drawn as shown in Fig. 7 for $[\delta z_1, \delta z_2, \delta z_3]_{\max} = [1, 1, 1]$ mm. In this work, we assume that the maximal input error of the mechanism is 1 mm. When the side length of reflector unit is equal to 7.5 m, the one-dimensional RMS fitting error is 3.75 mm.

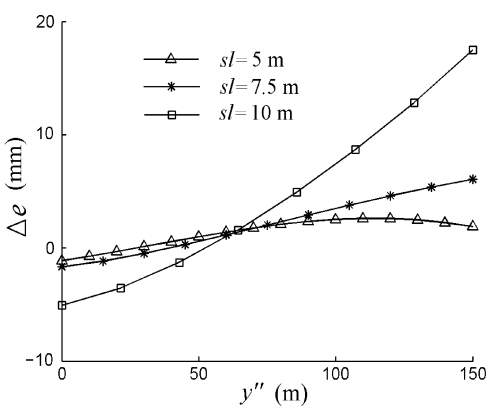

Fig. 6 Fitting error of reflector unit.

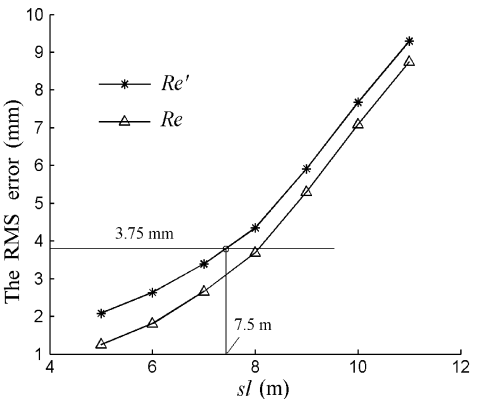

Fig. 7 One-dimensional RMS fitting error of active reflector.

5.2 Two-Dimensional Fitting Accuracy Analysis

As shown in Fig. 5a, the reflector unit fitting error is a closed region. In Section 5.1 we only considered the one-dimensional error. In this section the area of the closed region will be used to analyze and evaluate the fitting error, which is called the "two-dimensional fitting error". Obviously, the two-dimensional fitting error will provide a more reliable index when analyzing the fitting accuracy of the large spherical radio telescope. Figure 8 shows the two-dimensional fitting error of the ith reflector unit, which is the sectional region.

5.2.1 Circle Equation at Fitting Position

When reflector units are driven by the mechanisms, the circle arc equation of the ith reflector unit will be changed in the frame $\Re''$. As shown in Fig. 8, the centre of circle arc$A'_{i1}A'_{i3}A'_{i2}$ is changed from S to S'_i. The coordinate of S'_i in the frame $\Re$ is written as

$$[\mathbf{S'}_i]_{\Re} = [y_{S'i}, z_{S'i}]^{\mathrm{T}} = \mathbf{R}_1\,[\mathbf{S}]'_{\Re} + [y, z]^{\mathrm{T}}\,, \tag{30}$$

where

$$\mathbf{R}_1 = \begin{bmatrix} c\alpha & -s\alpha \\ s\alpha & c\alpha \end{bmatrix}, \quad [\mathbf{S}]'_{\Re} = [0, K]\,. \tag{31}$$

The coordinates of S'_i in the frame $\Re''$ are written as

$$[\mathbf{S}'_i]_{\Re''} = [y''_{S'i}, z''_{S'i}]^{\mathrm{T}} = \mathbf{R}_2\,[\mathbf{S}'_i]_{\Re} + [y''_{i3}, z''_{i3}]^{\mathrm{T}}\,. \tag{32}$$

The circle arc equation is changed to

$$z'' = K - \sqrt{K^2 - (y'' - y_{S'i})^2} + z''_{S'i} \quad . \tag{33}$$

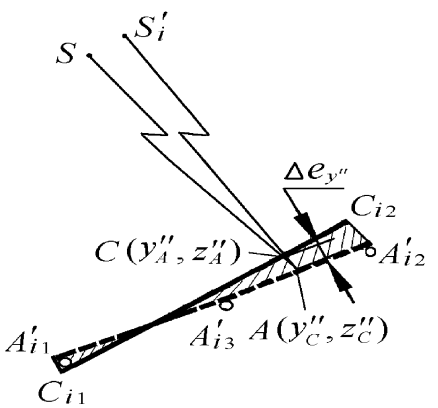

Fig. 8 Two-dimensional fitting error region of the ith reflector unit.

5.2.2 Two-Dimensional Fitting Error

The two-dimensional fitting error can be calculated according to the circle arc equation in the frame $\Re''$. First, as shown in Fig. 8, one point in the parabola is denoted as $C\,(y''_C, z''_C)$, the equation of the straight line SC can be written as

$$z'' = \frac{(z''_c - K)y''}{y''_c} + K \quad . \tag{34}$$

According to Eqs. (33) and (34), the point of intersection A between line SC and the circle arc $A'_{i1}A'_{i3}A'_{i2}$ can be expressed by $A\,(y''_A, z''_A)$. The fitting error of the given point is expressed as

$$\Delta e''_y = SA - SC = \sqrt{(y''_C - y''_A)^2 + (z''_C - z''_A)^2}. \tag{35}$$

The area of the closed region can be written as

$$Se_i = \int_{y''_{Ci1}}^{y''_{Ci2}} \left|\Delta e''_y\right| dy''\,, \tag{36}$$

which is the two-dimensional fitting error of the ith reflector unit. Then the average error of the two-dimensional fitting error is defined as

$$Qe_i = \frac{Se_i}{y''_{Ci2} - y''_{Ci1}} \quad . \tag{37}$$

Finally, the two-dimensional root-mean-square (RMS) fitting error of the paraboloid reflector is defined as

$$R_{Qe} = \sqrt{\frac{\sum_{i=1}^{n} Qe_i^2}{n}} \quad , \tag{38}$$

where n is the number of reflector units that make up the 300-meter aperture parabola.

5.2.3 Two-Dimensional Accuracy Synthesis Analysis

The two-dimensional accuracy synthesis analysis is defined as the composition RMS error caused by both the errors of the mechanism actuator input and of the two-dimensional fitting, and is denoted as R'_{Qe}. Eqs. (25), (34) and (35) can be used to calculate the two-dimensional composition RMS fitting error R'_{Qe}.

5.2.4 Simulation Example

The two-dimensional RMS error and composition RMS fitting error are shown in Fig. 9, where all the dimensional design parameters are the same as specified in Section 5.1.5. Comparing Figs. 9 and 8, we can learn that although both the one-dimensional and two-dimensional RMS fitting errors increase when the side length of the reflector unit increases, the two-dimensional RMS error is larger than one-dimensional RMS error.

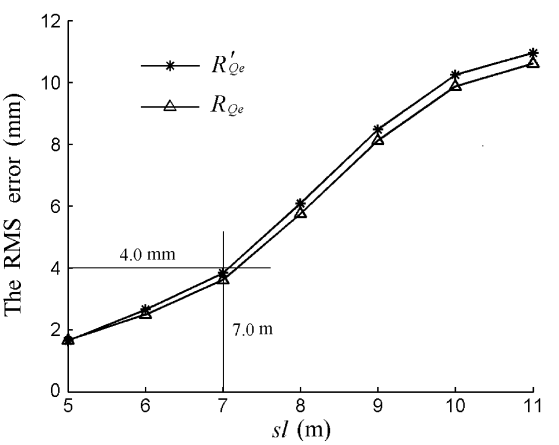

Fig. 9 Two-dimensional RMS fitting error of active reflector.

According to the fitting error requirement given by Qiu (1998), when the highest working frequency of the radio telescope is 5 GHz, the reflector RMS fitting error should be less than 3.75 mm. Now, we can assign the dimensional parameters and guarantee the implementation of the working frequency by the one-dimensional or two-dimensional RMS fitting error curves. For example, according to Fig. 8, if the side length of reflector unit is specified as 7.5 m, the specified dimension of reflector units can satisfy the requirement of 5 GHz working frequency. However, as shown in Fig. 9, if the two-dimensional RMS fitting error is used to evaluate the fitting accuracy, the side length of reflector unit should be less than 7.0 m to satisfy the requirement of 5 GHz working frequency.

6 CONCLUSIONS

For large spherical radio telescope application, a new active reflector supporting mechanism is proposed. The inverse kinematics is described in a closed form and the forward kinematics is also investigated. According to the analysis of one-dimensional and two-dimensional fitting errors, the conclusions can be drawn as follows: (1) The proposed mechanism can satisfy the motion requirements of the active reflector units; (2) The one-dimensional and two-dimensional fitting errors can be described as closed forms, and the relationship between the fitting errors and the design parameters of active reflector can be studied easily. (3) At the highest working frequency of 5GHz of the FAST, the hexagon dimension of the reflector unit should be less than 7 m in order to meet the required RMS accuracy.

The obtained results will be significant for the dimension design, trajectory plan and control of this type of mechanism.

Acknowledgements This piece of research is supported by the Fund of Large Radio Telescope Laboratory, National Astronomical Observatories, Chinese Academy of Sciences (No. Fast-B-06) and the State High-Technology Development Program of China (No. 2002AA421180).

References

Nan R. D., Peng B., 2000, Acta Astronautica, 46, 667
Qiu Y. H., 1998, MNRAS, 301, 827
Peng B., Nan R. D. et al., 2000, SPIE, 4015, 45
Li H., 1998, Science, 281, 771
Duan B. Y., 1999, Mechatronics, 9, 53
Luo Y. F., Deng C. G., Li G. Q., 2000, Journal of Tongji Univerisy, 28, 497
Wang J., Tang X., 2003, Journal of Machine Tool and Manufacture, 43, 647
Wang J., Tang X., Duan G., Li J., 2001, In: IEEE, The IEEE International Conference on Robotics and Automation, South Korea, 2448
Liu X. J, Wang J., Gao F., Wang L. P., 2001, IEEE Transactions on Robotics and Automation, 17, 959
Wang J., Liu X. J., 2003, Robotics and Autonomous Systems, 42, 31
Press W. H., Teukolsky S. A., Vetterling W. T., Flannery B. F., 1995, Numerical Recipes in C: The Art of Scientific Computing, 2nd Cambridge, U.K. Cambridge University Press